Journal of Nuclear Medicine, published on September 3, 2019 as doi:10.2967/jnumed.118.222513

Lesion Detection and Interobserver Agreement with Advanced Image-Reconstructions for ^{18}F-DCFPyL PET/CT in Patients with Biochemically Recurrent Prostate Cancer

Bernard H.E. Jansen[1,2], Robin W. Jansen[1], Maurits Wondergem[3], Sandra Srbljin[4], John M.H. de Klerk[5], Birgit I. Lissenberg-Witte[6], André N. Vis[2], Reindert J.A. van Moorselaar[2], Ronald Boellaard[1], Otto S. Hoekstra[1], Daniela E. Oprea-Lager[1]

[1]Department of Radiology & Nuclear medicine, Amsterdam University Medical Centers (VU University), the Netherlands
[2]Department of Urology, Amsterdam University Medical Centers (VU University), the Netherlands
[3]Department of Radiology & Nuclear medicine, Noordwest Ziekenhuisgroep, Alkmaar, the Netherlands
[4]Department of Nuclear Medicine, Zaans Medisch Centrum, Zaandam, the Netherlands
[5]Department of Radiology & Nuclear Medicine, Meander medisch centrum, Amersfoort, the Netherlands
[6]Department of Epidemiology & Biostatistics, Amsterdam University Medical Centers (VU University), the Netherlands

First author
Bernard H.E. Jansen, MD, PhD candidate
De Boelelaan 1117, 1081 HV Amsterdam
T: 020-4446033
E: bh.jansen@vumc.nl

Corresponding author
Daniela E. Oprea-Lager, MD, PhD
De Boelelaan 1117, 1081 HV Amsterdam
T: 020-4444366
E: d.oprea-lager@vumc.nl

Running title: Advanced Reconstructions for PSMA PET
Word count: 4999

ABSTRACT

Biochemically recurrent prostate cancer (BCR) is the main indication to perform *prostate-specific membrane antigen* positron emission tomography/computed tomography (PSMA PET/CT). However, localizing a BCR with PSMA PET/CT remains challenging in patients with low prostate-specific antigen (PSA) values. Here, we studied the impact of advanced PET image-reconstruction methods on BCR localization and interobserver agreement with ^{18}F-DCFPyL PET/CT scans in patients with BCR and low PSA values. **Methods:** Twenty-four patients with BCR and a PSA <2.0 ng/ml were included. PET images were reconstructed with 4mm voxels and 2mm voxels, both with and without point-spread-functions (PSF). All scans were interpreted by four nuclear medicine physicians. Additionally, PET examinations of five patients with primary prostate cancer and confirmed *absence* of lymph node metastases (following lymph node dissection) were included, to assess the risk of introducing false-positive findings when using advanced reconstructions. BCR localization rates (scan positivity) were calculated based on consensus among our readers (≥three readers regarding a scan positive for BCR), as well as the individual scan interpretations of the readers. **Results:** In the consensus analysis, BCR localization rates were not higher using advanced reconstruction methods (62.5-66.7%) compared to the 4mm reconstruction (62.5%). Based on individual readings, however, more scans were positive using the 2mm (74.0%, 95% CI 65.0-82.9%)(*p*=0.027) and 2mm+PSF reconstruction (75.0%, 95% CI 66.2-83.8%)(*p*=0.014) compared to the 4mm reconstruction (65.6%, 95% CI 56.0-75.3%). A higher number of lesions was detected on the 2mm (median 2 lesions, interquartile range 1-3) compared to 4mm scans (median 1, interquartile range 0-3; *p*=0.008). The advanced reconstructions methods did not increase interobserver agreement (80.6-84.7%), compared to the 4mm scans (75.7%, *p*=0.08-0.25). In the patients with primary PCa, an equal number of false-positive lesions was observed among the different reconstruction methods (overall *n*=13). **Conclusion:** Applying advanced image-reconstructions for ^{18}F-DCFPyL PET/CT scans did not increase BCR localization in patients with BCR and low PSA values (reader consensus). Yet, the increased number of positive individual readings may imply that further development of image-reconstruction methods holds potential to

improve BCR localization. No improved interobserver agreement was observed with advanced reconstruction compared to standard 4mm reconstructions.

Keywords: prostate cancer; ^{18}F-DCFPyL; image-reconstructions; PSMA

INTRODUCTION

Prostate cancer (PCa) is the most common cancer in men in the Western world(*1,2*). Since the introduction of tracers that bind the *prostate-specific membrane antigen* (PSMA), Positron emission tomography/computed tomography (PET/CT) is increasingly used for PCa diagnostics. PSMA is a class II trans-membrane glycoprotein that provides a valuable target for radiolabeled imaging, as it is significantly overexpressed in malignant prostate cells(*3*).

Currently, the main indication for PSMA PET imaging is the localization of biochemically recurrent prostate cancer (BCR) after initial therapy with curative intent(*4*). BCR is defined by two consecutive *prostate-specific Antigen* (PSA) values ≥0.2 ng/mL after radical prostatectomy, or any PSA 2.0ng/ml above the nadir after radiation therapy(*5,6*). Early lesion localization of BCR is desired for directing further treatment, which might include targeted radiotherapy or surgery(*6*). For the localization of BCR, [^{68}Gallium] labelled PSMA tracers ([^{68}Ga]PSMA-HBED-CC) appear promising(*4,7,8*). Alternatively, [^{18}Flourine] labelled PSMA tracers have been developed, most notably ^{18}F-DCFPyL(*9,10*) and ^{18}F-PSMA-1007(*11*). Due to a shorter positron range and higher positron yield, the ^{18}F-radionuclide provides a higher PET-image resolution than [^{68}Ga], which may improve detection of small metastases(*4*). Indeed, ^{18}F-DCFPyL PET/CT revealed enhanced localization of BCR compared to [^{68}Ga]PSMA PET/CT in first clinical analyses(*12,13*).

PET acquisitions can be reconstructed using various image-reconstruction methods. Typically, images are created with a voxel size of around 4mm(*14-16*). However, modern PET technique and reconstruction algorithms allow images with a higher resolution, resulting in voxels of 2mm. Additionally, reconstruction algorithms may include point-spread-functions (PSF), which could increase the spatial resolution and signal-to-noise ratio(*17,18*). For PSMA PET, these advanced image-reconstruction methods may influence the detection of (small) lesions suspicious for BCR – especially when using a ^{18}F-labelled tracer. This may be especially relevant for patients with BCR and a low PSA (<2.0ng/ml), in whom lesion detection with PSMA PET could still be improved (localization rates 11-80%)(*7,12,15*). Hence, the aim of this study was to evaluate if

advanced PET image-reconstructions for ^{18}F-DCFPyL PET/CT affect lesion detection in patients with BCR and low PSA values.

Limited information is available regarding the interobserver agreement of PSMA PET interpretation, which is a prerequisite for the acceptance of any imaging technique. Therefore, this study additionally assessed the interobserver agreement on ^{18}F-DCFPyL PET/CT interpretation and studied the effect of different image-reconstructions on agreement. For this assessment we included the proposed standardized interpretation systems PSMA-Reporting and Data System (PSMA-RADS)(*19*) and Prostate Cancer Molecular Imaging Standardized Evaluation (PROMISE)(*20*).

METHODS

Design

This is a comparative analysis of different image-reconstructions (4mm, 2mm, and PSF reconstructions) for ^{18}F-DCFPyL PET/CT scans in patients with BCR, using single-center data interpreted by four nuclear physicians from different centers.

The study has been approved by the institutional review board of the Amsterdam Medical Centers and the need for written informed consent was waived (review number 2018.453).

Patient Population

Twenty-four consecutive patients were retrospectively included from a single center (Amsterdam University Medical Centers, VU University). Inclusion criteria were: (1) newly detected BCR after radical prostatectomy; (2) current PSA of <2.0ng/ml; (3) availability of a ^{18}F-DCFPyL PET/CT scan. Patients were excluded if they received androgen deprivation therapy or other oncological treatment at the time of the ^{18}F-DCFPyL PET/CT scan.

Histologic verification of PSMA PET findings for BCR (e.g. through histological biopsy) is often difficult and therefore scarcely performed. Advanced image-reconstructions may offer early detection of PCa lesions, but might also result in false-positive findings. To assess the (added) risk of false-positive findings when using advanced reconstructions, we additionally included five primary PCa patients. Inclusion criteria for these patients were (1) histologically confirmed PCa (2) treated with radical prostatectomy in combination with extended lymph node dissection; (3) availability of a pre-operative ^{18}F-DCFPyL PET/CT scan; (4) confirmed *absence* of lymph node metastases on histopathological examination. Given the absence of nodal metastases, any suspect lymph node detected with ^{18}F-DCFPyL PET/CT (any reconstruction) was considered a false-positive result.

Imaging Protocol and Image-Reconstruction Methods

Routine clinical PET examinations were obtained from the Amsterdam UMC and included a low-dose CT scan (30mAs, 120kV). ^{18}F-DCFPyL was synthesized under GMP conditions at our own department (Radionuclide Center, Amsterdam UMC), using the precursor of ABX (ABX GmbH®, Germany). The median administered dose of ^{18}F-DCFPyL was 314.4 MBq (range 257.7-328.6 MBq), with a median uptake time of 120 minutes (range 99-142). No diuretics were administered prior to the scan. Imaging was performed with a hybrid Philips Ingenuity TF scanner (Philips Healthcare®, the Netherlands/USA)(crystal size 4x4x22 mm^3; 18 cm axial field-of-view; system sensitivity 7.3 cps kBq^{-1})(*21,22*). The scan trajectory included mid-thighs to skull vertex (4 minutes per bed position, 50% overlap). Images were corrected for decay, scatter, and random coincidences; photon attenuation was performed using low-dose CT.

The default BLOB-based Ordered-Subsets Expectations Maximization with Time-of-Flight reconstruction algorithm was used (3 iterations; 33 subsets)(*23*). For every PET examination (for the patients with BCR and primary PCa alike), images with 4x4x4 mm voxels, as well as 2x2x2 mm voxels were reconstructed (matrix size 144×144, slice thickness 4mm; matrix size 288x288, slice thickness 2mm). Both these 4mm and 2mm reconstructions were subsequently performed including PSF. The reconstruction methods are referred to as *4mm*, *4mm+PSF*, *2mm*, *2mm+PSF*. An illustration of the four image-reconstructions is presented in Fig. 1.

Image Interpretation

Scan interpretation was performed independently by four nuclear medicine physicians from different institutes (DO, MW, SS, JK), all with ample experience in ^{18}F-DCFPyL PET scan reading (>200 scans). All scans were anonymized and presented in a random order during 5 reading sessions over several months' time. The readers were blinded to clinical data, except for the indication of the scan (primary staging or BCR).

Specifically, the readers were unaware that the patients scanned for primary staging all had a confirmed *negative* lymph node status.

The readers assessed whether suspicious lesions were present in the prostate bed, lymph nodes, bone or visceral organs (routine clinical evaluation); they considered a scan 'positive' if at least one lesion suggestive of BCR was detected. For all individual lesions, a Likert score was given to assess readers' diagnostic confidence (1=PCa very unlikely; 2=PCa unlikely; 3=unclear/PCa possible; 4=PCa likely; 5=PCa very likely). In the first 12 BCR patients and the 5 primary PCa patients, the readers were additionally asked to characterize all lesions using the standardized classifications systems PSMA-RADS(*19*) and PROMISE(*20*). In short, the PSMA-RADS identifies five categories (PSMA-RADS 1-2 'benign'; PSMA-RADS 3 'equivocal'; PSMA-RADS 4-5 'likely PCa') based on PSMA uptake as well as a list of predefined findings on conventional imaging(*19*). In the PROMISE system, lesions are given an 'expression score' (*i.e.* tracer uptake is equal or higher than the blood pool, liver or salivary glands). With these scores, flowcharts can be consulted to classify a lesion as 'positive', 'equivocal' of 'negative'(*20*).

Statistical Analysis

Numerical variables were summarized with their means, median values and ranges; categorical variables with proportions (%), including 95% confidence intervals (CI). The four interpretations of the readers were gathered per scan. Final scan positivity was based on the existence of a consensus among the readers, which was defined as at least three readers detecting one or more lesions suggestive of BCR. The scan positivity rates of advanced reconstructed were compared to the 4mm reconstruction method ('clinical standard'). Additionally, the scan positivity rate and the average number of detected lesions were calculated per reconstruction method, based on all individual readings. Differences between reconstruction methods (individual readings) were compared in a repeated measures analysis using generalized linear mixed models (binary logistic model [scan positivity rate] and poisson loglinear model [number of lesions], with the

observers as within-subject variable and the reconstruction methods as fixed effect)(Supplemental Text). For the primary staging scans, only the individual readings were assessed, as the question here was how frequent false-positive findings are reported by individual readers.

To assess interobserver variability, the proportion of agreement was calculated(*24*). Differences in agreement per reconstruction method were analyzed with the generalized linear mixed models as described above. Significance level was set at p=0.05. Statistical modelling was performed with STATA © version 14.

RESULTS

BCR Localization Rates

The included patients with BCR had a median PSA value of 0.7 ng/ml (Table 1). Based on the consensus scores, no substantial differences were observed in the scan positivity rate of advanced reconstruction methods compared to the 4mm scans (Table 2). However, based on individual readings, more scans were positive using the 2mm (74.0%, CI 65.0-82.9%)(p=0.027) and 2mm+PSF reconstruction (75.0%, CI 66.2-83.8%)(p=0.014) compared to the 4mm reconstruction (65.6%, CI 56.0-75.3%). A higher number of lesions was detected on the 2mm (median 2 lesions, interquartile range 1-3) compared to 4mm scans (median 1, interquartile range 0-3; p=0.008) (Table 2).

Most scans were positive due to suspicious lymph nodes (38.8% of all scans) or recurrences in the prostate bed (27.6%) (Table 3). The extra positive scan interpretations (individual readings) with the 2mm and 2mm+PSF reconstructions mostly included additional identification of lesions in the prostate bed (n=7 out of 13 scan evaluations that were positive only with the 2mm or 2mm+PSF reconstruction). See Fig. 2 for illustrations.

Interobserver Agreement of BCR Scans

The advanced scan reconstructions did not significantly enhance interobserver agreement in this study (proportional agreement of 82.6-84.7% with the advanced reconstructions versus 78.5% with 4mm reconstructions) (Table 4). The positive agreement (83.6-89.8%) was higher than the negative agreement (66.7-74.7%) in all reconstructions (Table 4).

Primary Staging

In total, n=13 suspicious observations outside the prostate were described in any of the individual scan interpretations. In one patient, a single suspicious left femur bone lesion was described by three readers,

in all four image-reconstructions (*n*=12 observations). The single other detected lesion involved a suspect lymph node, observed only by one reader, in a 4mm+PSF scan. For both patients, the PSA levels after radical prostatectomy remained undetectable, suggesting that the observed lesions comprised false-positive results (current PSA follow-up 14 months and 10 months, respectively). All other scans were negative for metastatic PCa.

Lesion Characterization using Standardized Classification Systems

An overview of the scores of individual lesions is given in Table 5. The PSMA-RADS score was equal to the Likert score in 86.8% of all lesions (452/521). The PROMISE conclusion was equal to the Likert score in 91.4% of lesions (476/521) when the PROMISE score 'equivocal' and Likert score 3 were interpreted as positive (the PROMISE protocol hardly appoints equivocal scores). Different scores were primarily observed for lesions with a Likert score 1-3. Of all lesions with a Likert score 1-2 (PCa unlikely), 26.3% (10/38 lesions) were scored *positive* using PROMISE and 57.9% (22/38) scored *equivocal* using PSMA-RADS. Of all lesions with a Likert score 3 (PCa possible), 67.6% (50/74 lesions) had a positive PROMISE outcome and 24.3% (18/74) had a positive PSMA-RADS score.

If scan positivity was only based on the PSMA-RADS (i.e. score 4-5 'positive'), instead of the readers' routine clinical evaluation, *n*=2 individual scan interpretations would be different (1.0% of the first 12 BCR scans; both evaluations would become positive). If scan-positivity was based on the PROMISE protocol, *n*=7 scan interpretations would be different (3.6%; *n*=2 scans would be positive, *n*=5 scans negative).

In one primary staging scan, a false-positive bone lesion was observed (see above). The lesion was mostly rated *equivocal* on the Likert scale (8 of 12 ratings was '3') as well as the PSMA-RADS (7 of 12 ratings '3'). Yet, using PROMISE, all 12 lesions were rated positive.

Interobserver Agreement of Lesion Characterization

All lesions that were described by two or more readers were identified. To avoid double counting of lesions in multiple image-reconstructions, only the 2mm scans were analyzed (most available lesions). *N*=31 lesions were identified (*n*=16 by four readers, *n*=8 by three readers, *n*=7 by 2 readers; total readings *n*=102). The proportion of overall agreement was 84.9% (CI 76.4-91.3%) using the Likert scale; 83.3% (CI 74.5-90.1%) with PSMA-RADS; and 93.7% (CI 87.0-97.6%) with PROMISE. The proportional agreement for the 'expression score', used in PROMISE, was 42.9% (CI 32.9-53.2%).

DISCUSSION

In this study, different image-reconstruction methods for ^{18}F-DCFPyL PET/CT scans were evaluated in terms of lesion detection and interobserver agreement, in patients with BCR and low PSA values. Based on reader consensus, no higher BCR localization rates were observed when using the advanced images reconstructions (2mm) compared to standard scans (4mm). The proportional interobserver agreement was higher with the advanced reconstruction methods (82.6-84.7%) compared to the 4mm scans (78.5%), but results were not statistically different (Table 4).

In clinical practice, PSMA PET scans are most often evaluated by a single, individual reader. When looking at the individual scan interpretations, the 2mm or 2mm+PSF reconstruction resulted in 8-9% more positive scan evaluations (absolute %), with an increased number of detected lesions (Table 2). Taken altogether, our data do not support a strong recommendation for any advanced reconstruction over the standard 4mm reconstruction. Yet, the increased number of positive individual readings may imply that further development of image reconstruction methods holds potential to improve BCR localization. It should be noted, that for every individual patient four different scans were created (four reconstructions). This limited the number of individual patients we could include, and thus the statistical power to detect differences in lesion detection. As such, our results may rather be considered as hypothesis generating, pointing towards increased resolution PSMA PET scans (2mm) to enhance diagnostics.

For the individual patient, increased BCR localization may be clinically relevant, as PSMA PET outcomes influence therapeutic decisions regarding salvage local interventions, metastases-directed therapy, or the initiation of systemic treatment(*6,25,26*). It should be highlighted, however, that improved detection of lesions alone does not necessarily improve patient outcomes. There is an evident need to assess the effect of PSMA PET-based treatment on clinical outcomes (e.g. time to start androgen deprivation therapy,

progression-free survival, overall survival)(*6,27*). We believe these prospective evaluations may incorporate the use of advanced reconstruction methods.

The scan positivity rate with 4mm scans observed in this study (63% in the consensus analysis; 66% based on individual interpretations) is in line with previous results using [^{68}Ga]PSMA PET/CT for patients with similar PSA values(*7,15*). The prior study on ^{18}F-DCFPyL PET/CT by Dietlein et al. (*12*), used an advanced reconstruction method was as well (2-3mm voxels, including PSF). It reported a comparable scan positivity rate as was found in our study with the 2mm+PSF scans for patients with similar PSA values (67% in consensus analysis; 75% based on individual readings).

An important limitation of many studies on PSMA PET for BCR is the lack of histopathologic confirmation of PSMA PET results(*7,12,15*). PSMA PET detected lesions are often smaller than 1 cm, making biopsy procedures difficult and burdensome for patients. Without knowing the exact number of PCa metastases, the true diagnostic accuracy of PMSA PET cannot be assessed, however (neither for regular scans, nor for advanced image-reconstructions). To estimate the (added) risk on false-positive findings when using advanced image-reconstructions, we included patients with confirmed absence of lymph node metastases. No increase in false-positive findings was observed in these patients when applying the advanced reconstructions. Although these outcomes are encouraging, it should be stressed that these result are only based on a small number of primary PCa patients. True histologic verification of additionally detected lesions with advanced image-reconstructions in our patients with BCR was not performed.

If histological confirmation is not possible, clinical follow-up can provide another means to confirm the nature of detected lesions. Although the follow-up period of this study is limited (often less than one year), some clinical observations are worth mentioning. In one patient, many (>5) bone metastases were suspected by all readers, in all image-reconstructions. These lesions were again reported on bone scintigraphy 2 months later, substantiating the metastatic nature of these lesions. In two other patients, the detected

lesions (a local recurrence and a suspicious bone lesion, respectively) were confirmed on follow-up ^{18}F-DCFPyL PET/CT scans afterwards. Further, one patient received radiation therapy targeted on a local recurrence in the prostate bed, which resulted in a substantial PSA decrease. This lesion was described by all readers on the 2mm scans, but missed by one on a 4mm scan. Another patient received routine, 'blind' radiotherapy on the prostate bed (the clinical PET interpretation was negative), followed by an immediate PSA decrease. In our study, a local recurrence was suspected in this patient on a 2mm scan. Clearly, these clinical observations come with many limitations of its own. However, together with the results in the primary staging scans, it may substantiate the validity of our findings – in the absence of a golden standard.

In our patients with BCR and low PSA values, we anticipated mainly detection of small lesions, which is thought to be enhanced by PSF(*17,21*). No improved diagnostic results were observed when using PSF, however. In this first evaluation of PSF for BCR localization, we have used only the standard PSF reconstruction settings. Potentially, further development may improve diagnostic outcomes, for it has been demonstrated that PSF benefits from thorough optimization of all reconstruction parameters to balance contrast recovery versus the induction of noise(*18*).

The interobserver agreement in this study appears generally satisfactory, although the relatively lower negative agreement scores (67-75%) might imply that dual reading (of negative scans) is still advisable(*16*). The use of standardized reading protocols had limited effect on scan interpretation ('positive' or 'negative'), as may be expected when the observer agreement is already satisfactory. On a lesion level, using the PROMISE protocol resulted in many positive (i.e. *malignant*) classifications (Table 4). The interobserver agreement for the proposed 'expression score' was low (43%), however, which causes concern regarding the many positive classifications. Our readers reported to feel uncomfortable with some positive classifications using PROMISE. This was illustrated by the false-positive findings in the primary PCa patients: all these lesions were rated 'equivocal' on routine clinical interpretation, but rated 'positive' using PROMISE.

Recently, Yin et al. presented follow-up data on ‘equivocal lesions’ (PSMA-RADS 3). In line with our experience, they conclude that clinically dubious lesions are ‘truly indeterminate’ and certainly not always cancer(*28*).

Our study has limitations regarding the analysis of interobserver agreement and, overall, we were unable to demonstrate a clear benefit of the PSMA-RADS or PROMISE protocol. The lack of histological characterization of individual lesions hampers accurate comparison of the classification systems. Lastly, our readers primarily reported the findings they found clinically relevant, i.e. potentially malignant. It is possible that dubious lesions were described by some readers (who interpreted the lesions as malignant), but omitted by others (who interpreted the lesions as benign). Such lesions would consequently not be included in the interobserver agreement analysis, inflating our results on agreement on a lesion base.

CONCLUSION

In this study we evaluated the impact of advanced image-reconstruction methods for ^{18}F-DCFPyL PET/CT on lesion detection and interobserver agreement, in patients with biochemically recurrent prostate cancer and low PSA values. Based on reader consensus, the advanced image-reconstruction methods did not result in higher BCR localization rates. Yet, an increased number of positive individual scan interpretations was observed when using 2mm scans, implying further development of image reconstruction methods may hold potential to improve BCR localization. Given our limited sample size, future research is warranted to confirm these results. No improved interobserver agreement was observed with advanced reconstructions compared to standard 4mm reconstructions.

ACKNOWLEDGEMENTS

This study was supported by an unrestricted grant from Astellas Pharma B.V., the Netherlands.

DISCLOSURES

R. Boellaard reports to have a scientific collaboration with Philips Healthcare. The other authors have no disclosures or potential conflicts of interest to this manuscript.

REFERENCES

1. Ferlay J, Soerjomataram I, Dikshit R, et al. Cancer incidence and mortality worldwide: sources, methods and major patterns in GLOBOCAN 2012. *Int J Cancer.* 2015;136:E359-386.

2. Siegel RL, Miller KD, Jemal A. Cancer statistics, 2018. *CA Cancer J Clin.* 2018;68:7-30.

3. Perner S, Hofer MD, Kim R, et al. Prostate-specific membrane antigen expression as a predictor of prostate cancer progression. *Hum Pathol.* 2007;38:696-701.

4. Rowe SP, Gorin MA, Allaf ME, et al. PET imaging of prostate-specific membrane antigen in prostate cancer: current state of the art and future challenges. *Prostate Cancer Prostatic Dis.* 2016;19:223-230.

5. Amling CL, Bergstralh EJ, Blute ML, Slezak JM, Zincke H. Defining prostate specific antigen progression after radical prostatectomy: what is the most appropriate cut point? *J Urol.* 2001;165:1146-1151.

6. Cornford P, Bellmunt J, Bolla M, et al. EAU-ESTRO-SIOG Guidelines on Prostate Cancer. Part II: Treatment of Relapsing, Metastatic, and Castration-Resistant Prostate Cancer. *Eur Urol.* 2017;71:630-642.

7. Perera M, Papa N, Christidis D, et al. Sensitivity, Specificity, and Predictors of Positive 68Ga-Prostate-specific Membrane Antigen Positron Emission Tomography in Advanced Prostate Cancer: A Systematic Review and Meta-analysis. *Eur Urol.* 2016;70:926-937.

8. Afshar-Oromieh A, Zechmann CM, Malcher A, et al. Comparison of PET imaging with a (68)Ga-labelled PSMA ligand and (18)F-choline-based PET/CT for the diagnosis of recurrent prostate cancer. *Eur J Nucl Med Mol Imaging.* 2014;41:11-20.

9. Chen Y, Pullambhatla M, Foss CA, et al. 2-(3-{1-Carboxy-5-[(6-[18F]fluoro-pyridine-3-carbonyl)-amino]-pentyl}-ureido)-pen tanedioic acid, [18F]DCFPyL, a PSMA-based PET imaging agent for prostate cancer. *Clin Cancer Res.* 2011;17:7645-7653.

10. Szabo Z, Mena E, Rowe SP, et al. Initial Evaluation of [(18)F]DCFPyL for Prostate-Specific Membrane Antigen (PSMA)-Targeted PET Imaging of Prostate Cancer. *Mol Imaging Biol.* 2015;17:565-574.

11. Giesel FL, Hadaschik B, Cardinale J, et al. F-18 labelled PSMA-1007: biodistribution, radiation dosimetry and histopathological validation of tumor lesions in prostate cancer patients. *Eur J Nucl Med Mol Imaging.* 2017;44:678-688.

12. Dietlein F, Kobe C, Neubauer S, et al. PSA-stratified performance of 18F- and 68Ga-labeled tracers in PSMA-PET imaging of patients with biochemical recurrence of prostate cancer. *J Nucl Med.* 2016.

13. Wondergem M, Jansen BHE, van der Zant FM, et al. Early lesion detection with (18)F-DCFPyL PET/CT in 248 patients with biochemically recurrent prostate cancer. *Eur J Nucl Med Mol Imaging.* 2019;46:1911-1918.

14. Boellaard R, Delgado-Bolton R, Oyen WJ, et al. FDG PET/CT: EANM procedure guidelines for tumour imaging: version 2.0. *Eur J Nucl Med Mol Imaging.* 2015;42:328-354.

15. Afshar-Oromieh A, Holland-Letz T, Giesel FL, et al. Diagnostic performance of 68Ga-PSMA-11 (HBED-CC) PET/CT in patients with recurrent prostate cancer: evaluation in 1007 patients. *Eur J Nucl Med Mol Imaging.* 2017;44:1258-1268.

16. Burggraaff CN, Cornelisse AC, Hoekstra OS, et al. Interobserver agreement of interim and end-of-treatment (18)F-FDG PET/CT in diffuse large B-cell lymphoma (DLBCL): impact on clinical practice and trials. *J Nucl Med.* 2018.

17. Andersen FL, Klausen TL, Loft A, Beyer T, Holm S. Clinical evaluation of PET image reconstruction using a spatial resolution model. *Eur J Radiol.* 2013;82:862-869.

18. Akamatsu G, Ishikawa K, Mitsumoto K, et al. Improvement in PET/CT image quality with a combination of point-spread function and time-of-flight in relation to reconstruction parameters. *J Nucl Med.* 2012;53:1716-1722.

19. Rowe SP, Pienta KJ, Pomper MG, Gorin MA. Proposal for a Structured Reporting System for Prostate-Specific Membrane Antigen-Targeted PET Imaging: PSMA-RADS Version 1.0. *J Nucl Med.* 2018;59:479-485.

20. Eiber M, Herrmann K, Calais J, et al. Prostate Cancer Molecular Imaging Standardized Evaluation (PROMISE): Proposed miTNM Classification for the Interpretation of PSMA-Ligand PET/CT. *J Nucl Med.* 2018;59:469-478.

21. van der Vos CS, Koopman D, Rijnsdorp S, et al. Quantification, improvement, and harmonization of small lesion detection with state-of-the-art PET. *Eur J Nucl Med Mol Imaging.* 2017;44:4-16.

22. Kolthammer JA, Su KH, Grover A, Narayanan M, Jordan DW, Muzic RF. Performance evaluation of the Ingenuity TF PET/CT scanner with a focus on high count-rate conditions. *Phys Med Biol.* 2014;59:3843-3859.

23. Popescu LM, Matej S, Lewitt RM. Iterative image reconstruction using geometrically ordered subsets with list-mode data. Paper presented at: Nuclear Science Symposium Conference Record, 2004 IEEE, 2004.

24. de Vet HC, Mokkink LB, Terwee CB, Hoekstra OS, Knol DL. Clinicians are right not to like Cohen's kappa. *BMJ.* 2013;346:f2125.

25. Emmett L, van Leeuwen PJ, Nandurkar R, et al. Treatment Outcomes from (68)Ga-PSMA PET/CT-Informed Salvage Radiation Treatment in Men with Rising PSA After Radical Prostatectomy: Prognostic Value of a Negative PSMA PET. *J Nucl Med.* 2017;58:1972-1976.

26. Grubmuller B, Baltzer P, D'Andrea D, et al. (68)Ga-PSMA 11 ligand PET imaging in patients with biochemical recurrence after radical prostatectomy - diagnostic performance and impact on therapeutic decision-making. *Eur J Nucl Med Mol Imaging.* 2018;45:235-242.

27. Lecouvet FE, Oprea-Lager DE, Liu Y, et al. Use of modern imaging methods to facilitate trials of metastasis-directed therapy for oligometastatic disease in prostate cancer: a consensus recommendation from the EORTC Imaging Group. *Lancet Oncol.* 2018;19:e534-e545.

28. Yin Y, Werner RA, Higuchi T, et al. Follow-Up of Lesions with Equivocal Radiotracer Uptake on PSMA-Targeted PET in Patients with Prostate Cancer: Predictive Values of the PSMA-RADS-3A and PSMA-RADS-3B Categories. *J Nucl Med.* 2018.

TABLES & FIGURES

FIGURE 1: Example of the four image-reconstruction methods from a single patient. Maximum intensity projections and axial slides (identical scaling).

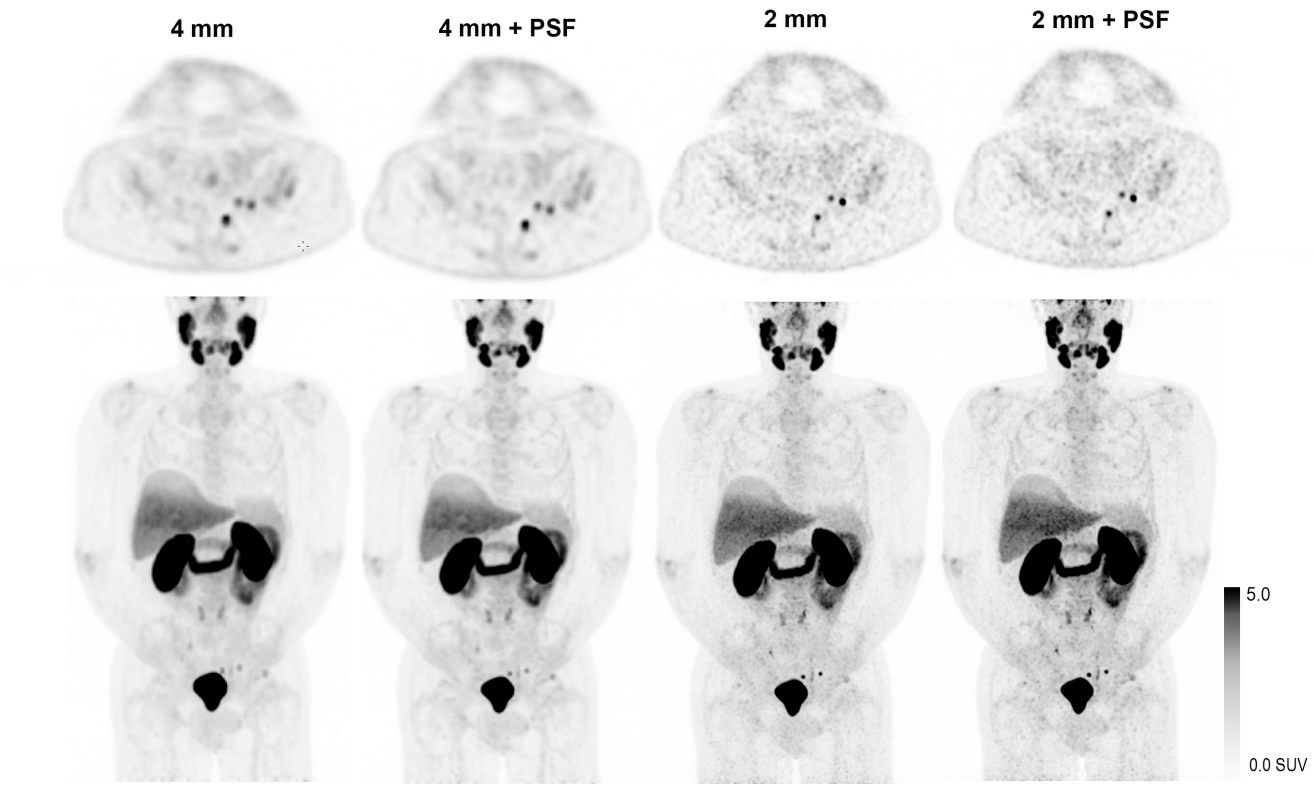

FIGURE 2: (A,B,C) Illustration of additional detection of local recurrences in three patients on 2mm scans (left) compared to 4mm scan (right).

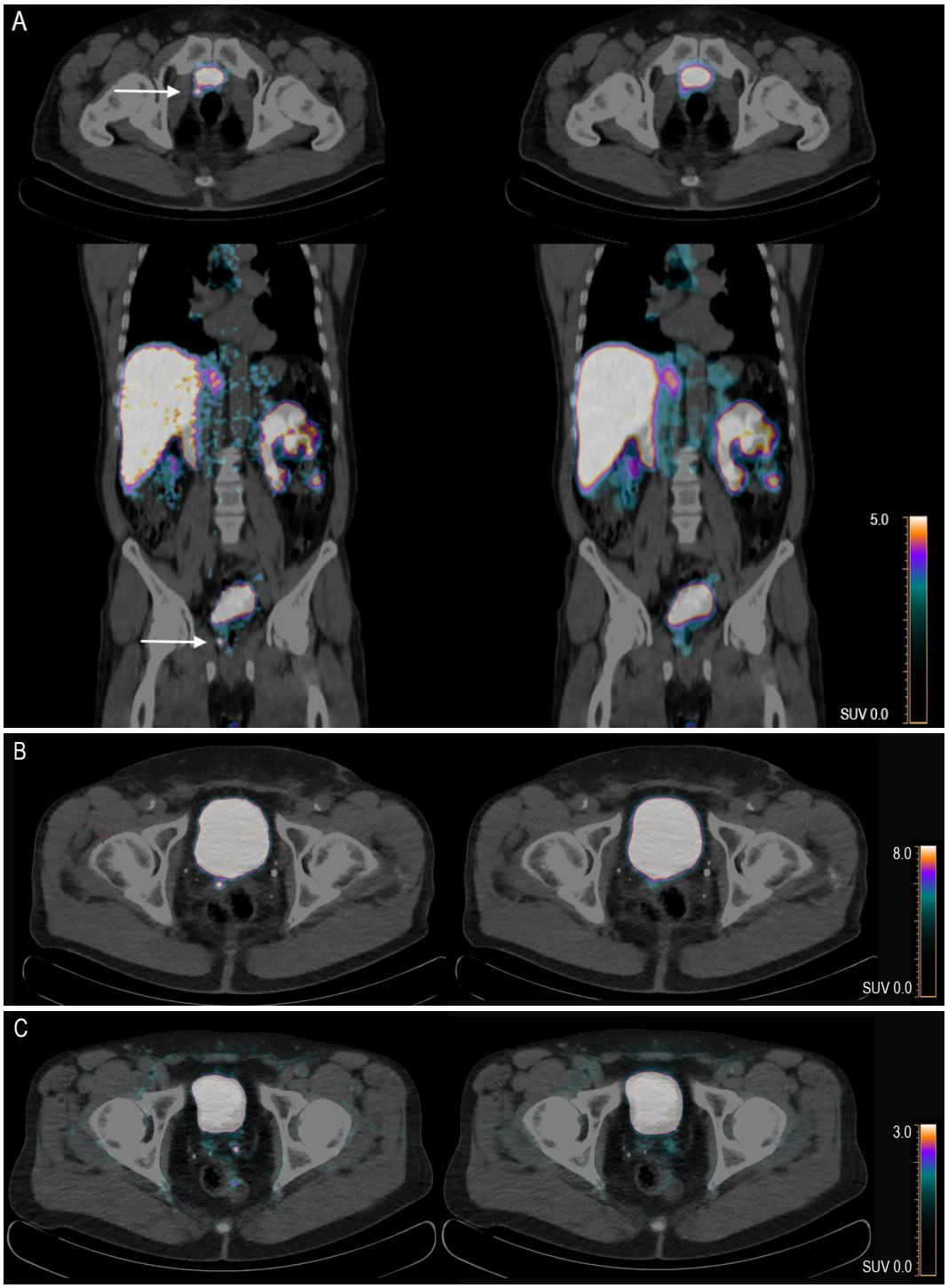

TABLE 1: Patient and scan characteristics

	BCR (*n*=24)		**Primary staging** (*n*=5)	
	median	*range*	*median*	*range*
Age (years)	67	61-77	63	55-69
PSA (ng/ml)	0.7	0.4-1.9	8.7	7.2-26.8
Gleason score [a]	7	6-9	7	7-8
Tumor stage [a]	3a	2a-4	3a	-
Injected dose (MBq)	314.3	257.7-328.6	318.8	299.0-325.9
Uptake time (minutes)	120	99-142	123	117-164
Inclusion period	Nov 2017 - Oct 2018		Nov 2017 - Feb 2018	

[a] *Based on prostatectomy specimens*

TABLE 2: Localization of BCR. Scan positivity rate; number of detected lesions

Reconstruction	Localization rate			Number of detected lesions			
	Consensus analysis (≥3 readers)	*95% CI*	*Individual readings*	*95% CI*	*mean*	*median*	*IQR*
4mm	15/24 (62.5%)	(41.6-83.4%)	63/96 (65.6%)	(56.0-75.3%)	2.2	1	(0-3)
4mm+PSF	15/24 (62.5%)	(41.6-83.4%)	63/96 (65.6%)	(56.0-75.3%)	2.1	1	(0-3)
2mm	16/24 (66.7%)	(46.3-87.0%)	71/96 * (74.0%)	(65.0-82.9%)	2.8 *	2	(1-3)
2mm+PSF	16/24 (66.7%)	(46.3-87.0%)	72/96 * (75.0%)	(66.2-83.8%)	2.4	1	(0-3)

** Significantly different from the 4mm reconstruction*

95% CI = 95% confidence interval

IQR = interquartile range

TABLE 3: Number of scan evaluations including one or more lesion(s), per anatomic location. Total number of lesions detected, per anatomic location.

Location	*N* scan evaluations	Total *N* lesions
Prostate bed	106 (27.6%)	106 (13.0%)
Lymph nodes	149 (38.8%)	454 (55.8%)
Bone	91 (23.7%)	241 (29.6%)
visceral	7 (1.8%)	7 (0.9%)
other / missing	3 (0.8%)	6 (0.7%)
no detected lesions	120 (31.3%)	

TABLE 4: Interobserver agreement scores, including 95%-confidence intervals

Reconstruction	Complete agreement [a]	Proportional agreement		
		Overall	*Positive agreement*	*Negative agreement*
4mm	14/24 (58.3%)	78.5% (69.8 - 85.7%)	83.6% (73.2 - 91.1%)	68.7% (51.9 - 82.5%)
4mm+PSF	16/24 (66.7%)	82.6% (74.4 - 89.1%)	86.8% (77.0 - 93.5%)	74.7% (58.4 - 87.2%)
2mm	16/24 (66.7%)	82.6% (74.4 - 89.1%)	88.3% (79.4 - 94.3%)	66.7% (47.1 - 82.8%)
2mm+PSF	18/24 (75.0%)	84.7% (76.8 - 90.8%)	89.8% (81.4 - 95.3%)	69.4% (49.5 - 85.2%)

[a] Equal interpretation (either positive or negative) of a scan by all four readers

TABLE 5: Lesion characterization using different interpretations protocols. Total numbers.
(Likert and PSMA-RADS categories 1-2 and 4-5 are taken together, i.e. PCa unlikely, PCa likely).

Likert score (*n*)	**PSMA-RADS**			**PROMISE**		
	1-2	*3A-D*	*4-5*	*negative*	*equivocal*	*positive*
1-2: PCa unlikely (*n*=38 [a])	15	22	0	25	1	11
3: unclear/PCa possible (*n*=74 [b])	2	53	18	22	2	50
4-5: PCa likely (*n*=409)	1	24	384	10	0	399

[a] 1 missing PSMA-RADS and PROMISE score; [b] 1 missing PSMA-RADS score

SUPPLEMENTAL TEXT: Log files of the data analyses
B. Lissenberg-Witte

For the analyses of the dichotomous scan result (variable `outcome` in print screen below), based on individual scan interpretations, the following syntax in STATA © 14 was used:

```
melogit outcome i.method || PIN: || observer:, or
```

For the analyses of the number of lesions (variable `Nlesions` in print screen below), the following syntax in Stata 14 was used:

```
mepoisson Nlesions i.method || PIN: || observer:, irr
```

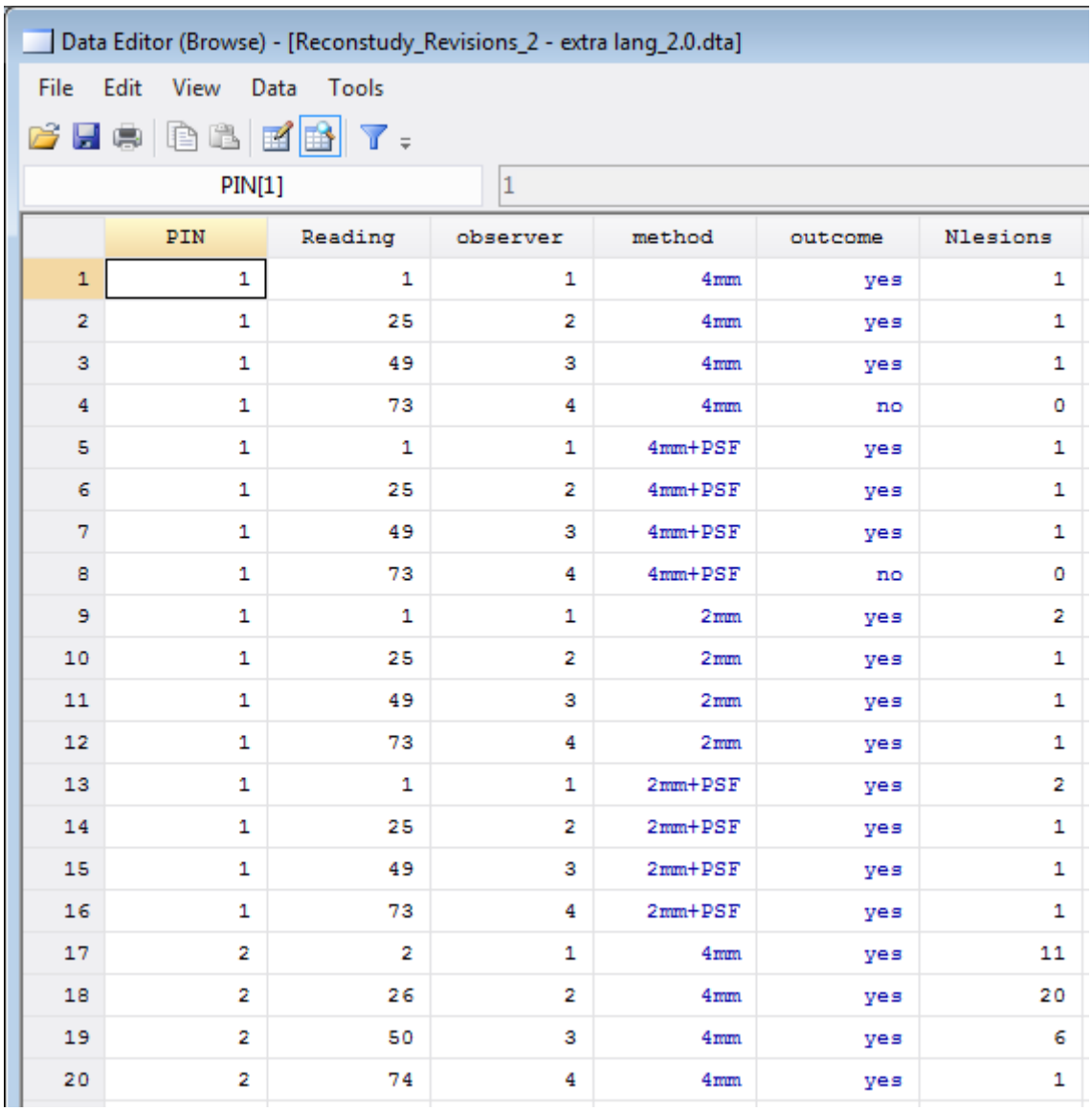

	PIN	Reading	observer	method	outcome	Nlesions
1	1	1	1	4mm	yes	1
2	1	25	2	4mm	yes	1
3	1	49	3	4mm	yes	1
4	1	73	4	4mm	no	0
5	1	1	1	4mm+PSF	yes	1
6	1	25	2	4mm+PSF	yes	1
7	1	49	3	4mm+PSF	yes	1
8	1	73	4	4mm+PSF	no	0
9	1	1	1	2mm	yes	2
10	1	25	2	2mm	yes	1
11	1	49	3	2mm	yes	1
12	1	73	4	2mm	yes	1
13	1	1	1	2mm+PSF	yes	2
14	1	25	2	2mm+PSF	yes	1
15	1	49	3	2mm+PSF	yes	1
16	1	73	4	2mm+PSF	yes	1
17	2	2	1	4mm	yes	11
18	2	26	2	4mm	yes	20
19	2	50	3	4mm	yes	6
20	2	74	4	4mm	yes	1

PIN=patient identification number

For the analyses of the agreement (variable `agree` in print screen below), the following syntax in Stata 14 was used:

```
melogit agree i.method || PIN: || pair:, or
```

Data Editor (Browse) - [Reconstudy_Revisions_2 - agreement_2.0.dta]

File Edit View Data Tools

PIN[1] 1

	PIN	method	pair	agree
1	1	4mm	12	yes
2	1	4mm	13	yes
3	1	4mm	14	no
4	1	4mm	23	yes
5	1	4mm	24	no
6	1	4mm	24	no
7	1	4mm+PSF	12	yes
8	1	4mm+PSF	13	yes
9	1	4mm+PSF	14	no
10	1	4mm+PSF	23	yes
11	1	4mm+PSF	24	no
12	1	4mm+PSF	24	no
13	1	2mm	12	yes
14	1	2mm	13	yes
15	1	2mm	14	yes
16	1	2mm	23	yes
17	1	2mm	24	yes
18	1	2mm	24	yes
19	1	2mm+PSF	12	yes
20	1	2mm+PSF	13	yes
21	1	2mm+PSF	14	yes
22	1	2mm+PSF	23	yes
23	1	2mm+PSF	24	yes
24	1	2mm+PSF	24	yes
25	2	4mm	12	yes
26	2	4mm	13	yes
27	2	4mm	14	yes
28	2	4mm	23	yes
29	2	4mm	24	yes
30	2	4mm	24	yes

PIN=patient identification number